JOURNAL OF ENGINEERING SCIENCES

Volume 11, Issue 2 (2024)

Babu J., Ramana M. V., Vivek D., Reddy C. H. S. (2022). Simultaneous optimization of delamination and thrust force during drilling of GFRP laminate with a core drill by E-PIV method. Journal of Engineering Sciences (Ukraine), Vol. 11(2), pp. A12–A21. https://doi.org/10.21272/jes.2024.11(2).a2

Simultaneous Optimization of Delamination and Thrust Force during Drilling of GFRP Laminate with a Core Drill by E-PIV Method

Babu J.[1*][0000-0003-3018-1327], Ramana M. V.[2], Vivek D.[2], Reddy C. H. S.[2]

[1] Department of Mechanical Engineering, IMPACT College of Engineering & Applied Sciences, 60 Feet Rd., Sahakara Nagar South, Kodigehalli, Koti Hosahalli, Bengaluru, 560092, Karnataka, India;
[2] Department of Mechanical Engineering, CVR College of Engineering, Ibrahimpatnam, Vastunagar, Mangalpalle, Hyderabad, 501510, Telangana, India

Article info:

Submitted:	March 22, 2024
Received in revised form:	June 28, 2024
Accepted for publication:	July 16, 2024
Available online:	July 24, 2024

***Corresponding email:**
jalumedi.babu@gmail.com

Abstract. Aeronautical applications are permanently improving because of the excellent mechanical capabilities of glass-fiber-reinforced polymers (GFRP). Drilling is a vital machining task required to put the structures made of these composites together. However, these GFRP composites need more precise machining than metallic materials. This machining procedure causes delamination in the composite composition. Delamination at the exit and entry of drilled holes is a severe problem for composite materials. By maximizing the controlling variables of the drilling process, superior-drilled holes can be generated. The present study aims to optimize the drilling settings by considering various performance aspects using the entropy weight-coupled proximity indexed value method. For this study, Taguchi's L25 5-level orthogonal array was employed. The responses are at the exit, entry delamination, and thrust force, while the control variables are feed rate and spindle speed. The findings indicate that more significant spindle speeds and smaller feed rates improve drilling success. Furthermore, current research indicates that feed rate has a more significant impact on the quality of the drilling holes.

Keywords: composites, equivalent delamination factor, energy efficiency, entropy, proximity indexed value method.

1 Introduction

Designers frequently use composites instead of traditional metallic materials in aerospace, automotive, and defense sectors, where structures with low weight, high strength, and stiffness are essential [1–2]. These materials have inherent properties, including limited heat conductivity, high heterogeneity and abrasive structure, and heat sensitivity, that make them difficult to process.

During the machining process, these materials display a range of defects, such as matrix cracking, deboning, and delamination [3–5].

Many scientists investigating GFRP composite drilling focused on thrust force and how it affects machining defects, specifically delamination.

A thorough explanation of delamination and the methods for measurement and assessment were given elsewhere [6–8].

2 Literature Review

Khashaba et al. [9–10] conducted empirical and analytical studies on the influence of machining conditions on GFRP composites, focusing on thrust force and delamination. The influence of production techniques on the mechanical properties of GFRP composite laminates was studied by Formisano et al. [11]. The studies of Erturk et al. [12] explore the influence of drilling conditions on the temperature and delamination of GFRP composite laminates, including feed rate, spindle speed, and drill bits.

Drill bit shape and coatings have been the subject of current research to reduce delamination and improve hole quality [13–15]. A few studies focused on the effects of exit temperatures [16–20] and tool wear [16] on surface degradation and delamination.

Another recent study focused on predicting thrust forces due to tool wear while drilling CFRP/Al stack [21] and

CFRP [22] unidirectional composites. Jai et al. [23, 24] comprehensively investigated delamination-free machining methods for CFRP composites. Research by Rahmé et al. [25] showed that delamination might be decreased by adding a woven glass sheet to the CFRP sheets' exit side of the drilled hole. A comprehensive study of bolted joints used to join fiber-reinforced composites was presented by Galinska et al. [26]. Several studies [19, 27] employed non-traditional techniques to reduce delamination damage while drilling composite materials. The drill bit tip angle is believed to affect thrust forces and delamination damage significantly [28]. Unintentional cutting angles are dispersed because of improper cutting-edge design, which degrades the material and reduces its cutting capacity, increasing thrust forces and delamination [29, 30]. The study by Durao et al. [31] on the effect of several drill bit geometries on delamination and thrust force indicates that step and dagger drills had the least thrust force.

Kilickap [32] investigated whether reducing the drill bit tip angle during GFRP sheet drilling could lessen delamination. Experimental and numerical studies by Dáz-Lvarez et al. [33] show that more substantial point angles result in stronger thrust forces while, on the other hand, reducing delamination damage. It has been analytically demonstrated by Ismail et al. [34] that as the chisel edge ratio increases, so do the feed rate and critical thrust forces. The effect of several drill bit geometries on the diameter deviation, surface roughness, and coaxial features of hole quality was investigated by Arrospide et al. [35]. The trials conducted by Liu et al. [36] demonstrate that the thrust forces generated by extruding the chisel edge were higher than those obtained by cutting it. The trials conducted by Liu et al. [36] demonstrate that the thrust forces generated by extruding the chisel edge were higher than those obtained by cutting it. Push-out delamination may be minimized or eliminated by milling CFRP laminates using a compounded, dragger, or candlestick drill, according to Qiu et al. [37]. According to Hocheng et al.'s investigations using a variety of drill bits, including twist, candlestick, saw, core, and step drills, the core drill permits the grater's critical feed; below this force, delamination that is expected will not occur [38–40].

Nekrasov S. et al. [41] proposed an innovative joint of FRP machine parts with a threaded connection with a rope thread made in reinforced composite material and could obtain the strength of the joint at a high level. Wang et al. [42] investigated the influence of the low-temperature drilling process on the mechanical behavior of CFRP. Their results showed that the mechanical properties of specimens with a low-temperature drilling process are lower than those of the specimen with a normal drilling process due to the better drilling quality. Wu et al. [43] studied the residual stresses in CFRP through the hole-drilling method. Their results revealed that the stacking sequence and overall dimensions of the CFRP samples significantly influence the residual stress state.

Babu J. et al. [7] studied the impact of feed and speed on delamination at the exit side of the hole drilled in GFRP composites using several delamination factor models, including the conventional delamination factor, adjusted delamination factor, and equivalent delamination factor. The results indicated that feed influences push-out delamination more. Using ANOVA and Taguchi's approach, Davim and Reis established a way to show the link between feed and speed on delamination in a composite lamina [8]. Palanikumar proposed an effective technique for optimizing drilling conditions (feed and speed) with several performance variables (surface roughness, thrust force, and delamination factor) by combining the Taguchi method with Grey Relational Analysis. The results of their study indicate that feed matters more than spindle speed [9].

Most studies conducted tests at three or four levels to determine the effect of drilling conditions on delamination while drilling composite laminate using Taguchi and ANOVA approaches [8–12]. The new work used Taguchi's L25 5-level orthogonal array in its trials, which is different from previous studies and should enhance the accuracy of the results. In these experiments, the control factors considered are feed and speed.

The main aim of this work is to optimize the drilling conditions during the GFRP composite drilling process by using a diamond-coated core drill that allows for a more significant critical thrust force. The Taguchi technique and hybrid optimization method are used in this process. The entropy method was used to calculate weights and then integrated with the proximity-indexed value method. Babu et al. [44] presented the most promising equivalent delamination factor to evaluate the delamination damage impacting the composite laminate around the hole's exit and entrance. This further increased the accuracy of the result. MINITAB 17 was utilized for both the design and analysis of drilling experiments to identify the key variables influencing the drilling of GFRP composites.

Early optimization studies in the literature either employed subject methods like the SIMO method or applied equal weightage to all responses. This may be an inappropriate or incorrect method to optimize the drilling parameters. To make a multi-objective problem into a single objective, known as E-PIV, the entropy approach, as an objective method, was combined with the proximity indexed value method to obtain the most scientific weights. The combination method can resolve complex multi-objective optimization issues [45, 46].

However, relationships with assessing replies are disregarded during this conversion procedure. This approach presents improved optimization by utilizing the proper weights for each response.

The specific objectives of this study are:

– optimizing the drilling conditions spindle speed and feed rate for minimum delamination and thrust force;

– use of the entropy method, which is an objective method for calculating the weights for accuracy of results;

– use of proximity indexed value method for simultaneous optimization of delamination and thrust force and its applicability in process optimization.

3 Research Methodology

3.1 Experimental procedure

Commercially available 26-layer GFRP composite laminates configured symmetrically in the form "0, 90" were used in this study. The applied resin was grade L-12 resin with K-5 hardener, and the fibers employed were bidirectional E-glass. The thickness of the laminate was 6 mm. A laminate was cut to the 250×40×6 mm^3 workpiece material sample size. According to Taguchi's L25 orthogonal array, drilling experiments were conducted on GFRP laminates using a 10 mm diamond-coated core drill. The minimum speed recommended for these drills for general purposes is 2000 rpm. The material used in this study is GFRP composite material. Hence, the present study uses spindle speeds ranging from 1500–2500 rpm to optimize the conditions for the chosen material. Feed rates are chosen correspondingly.

At PSG College of Engineering in Coimbatore, India, experiments were conducted with a computer numerical control (CNC) Makino Vertical Machining Centre (Model S33). Every experiment was conducted twice to lower the experimental error. The experimental setup with the dynamometer (Syscon SI-223D) is illustrated in Figure 1.

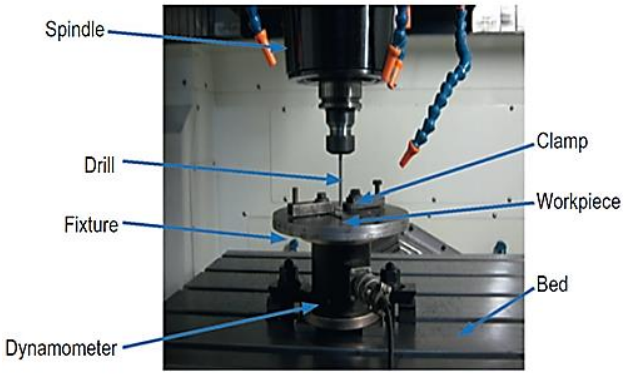

Figure 1 – Experimental setup

The dynamometer works based on strain gauge theory. The Wheatstone bridge circuit imbalance is caused by torque and thrust force levels that produce voltage commensurate with applied force and torque. A digital storage oscilloscope "Tektronix TDS210" was used to record and preserve the force and torque fluctuations during the drilling process. Push-out and peel-up delamination effects were also considered in the trials. Throughout all the trials, no coolant was used. Table 1 displays the drilling conditions considered for this study based on the literature [9].

Table 1 – Drilling parameters with their levels

Level	Feed, mm/min	Speed, rpm
1	50	1500
2	75	1750
3	100	2000
4	125	2250
5	150	2500

3.2 Measurement of delamination

While different researchers have employed many methods to evaluate the delamination of composites due to drilling, the most widely used ones include digital photography [16], ultrasonic C-scan [15], optical microscope [9–11], and X-ray [14]. Other methods of measuring delamination include acoustic emission [17] and shadow Moire laser-based imaging technology [18]. In a review publication, Babu et al. [6] thoroughly examine the delamination assessment techniques. The delamination damage at the drilled hole's entrance and exit was identified in this analysis using digital image processing techniques. The quantity of delamination was determined by scanning these drilled holes with a scanner that had a resolution of 1200 dpi. The scanned photos were put into the image-editing program Image J.

A picture of acceptable quality requires careful selection of several parameters, which are covered in more detail in [44, 47]. The main parameters include brightness intensity, image enhancement, noise suppression, and edge detection. The damage zone cannot be measured until the black and grey points in the binary image have been eliminated using the threshold filter. The Brightness intensity is adequately high to ensure clear visibility of the delamination region in the range of 500–1000 lux. This uniform and diffused lighting minimizes shadows and reflections on the GFRP surface. Image enhancement constitutes contrast adjustment to highlight the delaminated areas against the non-delaminated regions and histogram equalization to enhance the contrast of images, making the delamination more distinguishable. Median filtering of 5x5 pixels was used to reduce noise while preserving edges. Gaussian blur is applied with a low sigma value of $\sigma = 1$ to further smoothen the image without blurring significant features. Edge detection was done with Canny Edge Operator with a threshold typically set between 150–200. The processed image is then converted into a binary image where the delaminated areas are represented by white pixels and non-delaminated areas by black pixels. The number of white pixels is counted to quantify the delamination area using Image J analysis software.

The present investigation employs the effective equivalent delamination factor approach, as published by Babu et al. [44], to define the damage intensity to the composite material at the exit and entry sides of the hole. The approach is schematically depicted in Figure 2.

It is also can be computed as follows:

$$FEED = \frac{D_{ea} + D_{ep}}{D}, \quad (1)$$

where D_{ea} – the equivalent diameter of a circle whose size is equal to the region surrounded by the damaged zone's envelope:

$$D_{ea} = \sqrt{\frac{4A_e}{\pi}}, \quad (2)$$

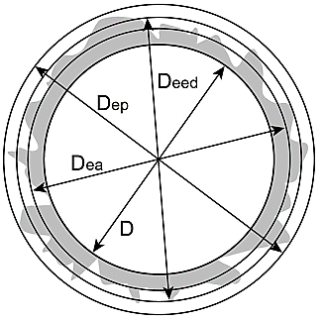

Figure 2 – Scheme of the effective equivalent delamination factor

The equivalent diameter of a circle whose perimeter length is equal to the envelope of the damaged zone:

$$D_{ep} = \frac{P_e}{\pi}, \quad (3)$$

Parameter D_{ep} represents the lengths of the cracks in the delamination. Parameter D_{ea} represents the area of damage caused by delamination. As a result, parameter D_{ep} will always be greater than D_{ea} and D.

Image J program allows for measuring the envelope's area and perimeter (Figure 3).

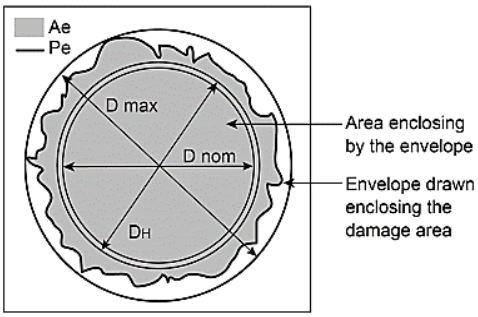

Figure 3 – The design scheme of P_e and A_e

4 Results

4.1 The main effects

Responses from the experiments are delamination at both push-out and peel-up, and thrust force for various drilling parameters are shown in Table 2.

With an increase in feed, delamination damage and thrust force also rise. Delamination and thrust force are connected phenomena; delamination grows in response to increased thrust force, and vice versa.

The characteristics of individual performance have been studied by several academics [8, 10–12]. Optimizing many performance parameters is necessary to increase production and improve the performance of manufactured components. The hardness, toughness, orientation, and flexibility of the fibers impacted the machining process of these composite materials [9].

Simultaneous optimization of several aspects is complicated for these composite materials. Drilling process parameters for GFRP composites are optimized for many performance variables.

Table 2 – Experimental design with responses

Exp. no	Speed, rpm	Feed, mm/min	Delamination factor		Thrust force, N
			Push-out	Peel-up	
1	1500	50	2.16	2.15	143.50
2	1500	75	2.19	2.17	246.00
3	1500	100	2.20	2.25	398.50
4	1500	125	2.21	2.26	522.50
5	1500	150	2.21	2.36	680.50
6	1750	50	2.14	2.14	103.00
7	1750	75	2.15	2.14	220.00
8	1750	100	2.16	2.15	334.00
9	1750	125	2.17	2.15	455.50
10	1750	150	2.21	2.15	586.00
11	2000	50	2.14	2.13	108.50
12	2000	75	2.14	2.14	203.00
13	2000	100	2.15	2.14	308.00
14	2000	125	2.16	2.15	406.50
15	2000	150	2.20	2.15	487.50
16	2250	50	2.12	2.13	67.00
17	2250	75	2.14	2.14	94.50
18	2250	100	2.16	2.16	145.50
19	2250	125	2.18	2.17	209.50
20	2250	150	2.22	2.23	255.00
21	2500	50	2.13	2.11	61.50
22	2500	75	2.17	2.15	96.50
23	2500	100	2.21	2.23	136.50
24	2500	125	2.26	2.28	180.50
25	2500	150	2.29	2.31	246.00

Drilling performance characteristics include delamination at the entry and exit, along with thrust and torque. Lower torque, delamination factor, and thrust force values are desirable for improved hole quality and the input settings for spindle speed and feed rate. Main effect graphs are used to examine how various variables affect GFRP composite machining.

The main effect plots for thrust force and delamination factor S/N ratios are displayed in Figures 4–6. Figure 4 shows how speed and feed affect thrust force during drilling. The results indicate that thrust force decreases with increasing speed. This happens because of growing speed, which increases the amount of heat that accumulates and softens the polymer matrix, decreasing thrust force. However, as the feed grows, so does the stress on the drill. This leads to higher thrust force and torque values while drilling composites. The impact of drilling settings on delamination damage at the entry and exit is depicted in Figures 5, 6.

The observed delamination factor is more likely to occur at high feed rates and low spindle speeds. Delamination and thrust force are connected phenomena; delamination grows in response to increased thrust force and vice versa.

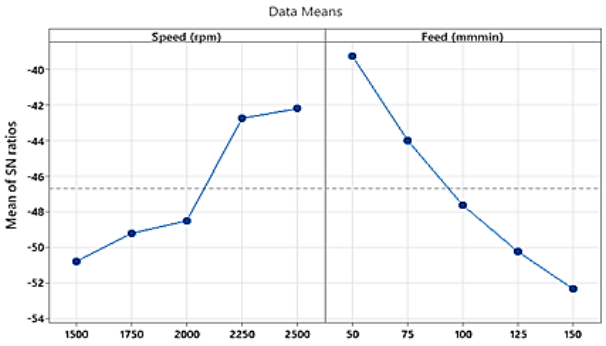

Figure 4 – The main effect plot for S/N ratios of thrust force

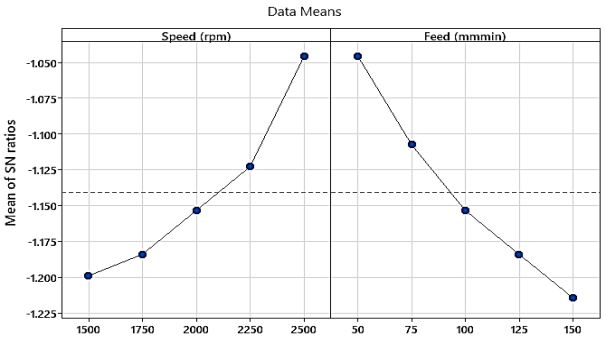

Figure 5 – The main effect plot for S/N ratios of peel-up delamination

4.2 Entropy method

The entropy values for each individual output response are calculated as follows:

$$e_j = -\frac{1}{lnm}\sum_{i=1}^{m} P_{ij}\, ln(P_{ij}), \qquad (4)$$

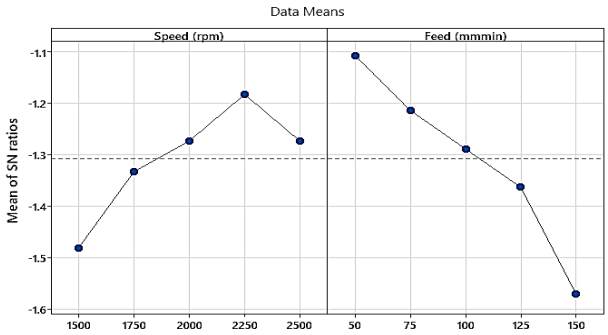

Figure 6 – Main effect plot for S/N ratios of push-out delamination

where $P_{ij} = \frac{y_{ij}}{\sum_{i=1}^{m} y_{ij}}$; $m = 25$ – the total number of experimental conditions. To normalize the data, the weights of responses are used:

$$w_j = \frac{1-e_j}{\sum_{i=1}^{n}(1-e_j)}. \qquad (5)$$

With respect to entropy values e_j, the performance response or characteristics are either growing or decreasing.

Entry, exit delamination factors, and thrust force had weights of 0.22, 0.33, and 0.45, respectively, which were calculated using equation (5).

Tables 3, 4 present the computed normalized performance characteristics P_{ij} and $ln(P_{ij})$ entropy values.

From Table 4, it can noticed that the entry delamination factor has a weightage of 0.22, whereas exit or push-out delamination and thrust force have higher weightages of 0.33 and 0.45, respectively.

Table 3 – $P_{ij}\, ln(P_{ij})$ values for output responses

Exp.	Normalized P_{ij}			P_{ij}			$P_{ij}\, ln(P_{ij})$		
no	*A*	*B*	*C*	*A*	*B*	*C*	*A*	*B*	*C*
1	0.278	0.250	0.135	0.029	0.026	0.016	–0.103	–0.094	–0.066
2	0.444	0.333	0.300	0.047	0.034	0.036	–0.143	–0.116	–0.119
3	0.500	0.714	0.546	0.052	0.074	0.065	–0.154	–0.192	–0.178
4	0.556	0.762	0.745	0.058	0.078	0.089	–0.165	–0.200	–0.215
5	0.556	1.238	1.000	0.058	0.127	0.119	–0.165	–0.263	–0.254
6	0.167	0.190	0.069	0.017	0.020	0.008	–0.071	–0.077	–0.040
7	0.222	0.190	0.258	0.023	0.020	0.031	–0.087	–0.077	–0.107
8	0.278	0.238	0.442	0.029	0.025	0.053	–0.103	–0.091	–0.155
9	0.333	0.238	0.637	0.035	0.025	0.076	–0.117	–0.091	–0.196
10	0.556	0.238	0.848	0.058	0.025	0.101	–0.165	–0.091	–0.232
11	0.167	0.143	0.078	0.017	0.015	0.009	–0.071	–0.062	–0.044
12	0.167	0.190	0.230	0.017	0.020	0.028	–0.071	–0.077	–0.099
13	0.222	0.190	0.400	0.023	0.020	0.048	–0.087	–0.077	–0.145
14	0.278	0.238	0.558	0.029	0.025	0.067	–0.103	–0.091	–0.181
15	0.500	0.238	0.689	0.052	0.025	0.082	–0.154	–0.091	–0.206
16	0.056	0.143	0.011	0.006	0.015	0.001	–0.030	–0.062	–0.009
17	0.167	0.190	0.056	0.017	0.020	0.007	–0.071	–0.077	–0.033
18	0.278	0.286	0.138	0.029	0.029	0.016	–0.103	–0.104	–0.068
19	0.389	0.333	0.241	0.041	0.034	0.029	–0.130	–0.116	–0.102
20	0.611	0.619	0.314	0.064	0.064	0.038	–0.176	–0.175	–0.123
21	0.111	0.048	0.002	0.012	0.005	0.000	–0.052	–0.026	–0.002
22	0.333	0.238	0.059	0.035	0.025	0.007	–0.117	–0.091	–0.035
23	0.556	0.619	0.123	0.058	0.064	0.015	–0.165	–0.175	–0.062
24	0.833	0.857	0.194	0.087	0.088	0.023	–0.213	–0.214	–0.087
25	1.000	1.000	0.300	0.105	0.103	0.036	–0.236	–0.234	–0.119
The sum of $\sum_{i=1}^{m} P_{ij} \ln(P_{ij})$							–3.05	–2.96	–2.87

Table 4 – Weights of the responses using the entropy method

Response	e_j	$1 - e_j$	w_j
A	0.9455	0.0545	22
B	0.9176	0.0824	33
C	0.8897	0.1103	45
	Sum	0.0612	100

4.3 Proximity indexed value method

Methodology for process optimization using proximity indexed value (PIV) method [45]. This method has recently been used to solve the problems of process, material, and supplier selection [46].

Step 1: Define the process optimization problem

Step 2: Determining the number of experiments with process parameters P_i (i = 1, 2, …, m) and determining the output responses Q_j (j = 1, 2, …, n).

Step 3: Determining criteria weights by an appropriate method. In this problem, the entropy method was used.

Step 4: Preparation of a decision matrix X, the experiments with process parameters in rows, and the corresponding output responses in columns as follows [48]:

$$\mathbf{R} = \begin{vmatrix} r_{ij} & r_{12} & r_{13} \\ r_{21} & r_{22} & r_{23} \\ r_{31} & r_{32} & C_{33} \end{vmatrix}. \quad (6)$$

Step 5: Decision matrix normalization [48]:

$$r_{ij}^* = \frac{r_{ij}}{\sqrt{\sum_1^m r_{ij}^2}}, \quad (7)$$

where r_{ij} – the i-th experiment condition j-th response; m, n – the numbers of experiments and output responses.

Step 6: Determining the weighted-normalized decision matrix [48]:

$$V_{ij} = r_{ij}^* X\, W_j, \quad (8)$$

where r_{ij}^* – normalized number for i-th experiment condition of j-th response; W_j – the weightage of the response.

Step 7: Calculation of weighted-proximity index value [48]:

$$u_i = \begin{cases} V_{max} - V_i \ \ for\ beneficial\ criteria; \\ V_i - V_{min} \ \ for\ cost\ criteria. \end{cases} \quad (9)$$

Step 8: Determination of overall proximity value [48]

$$d_i = \sum_1^m u_i, \quad (10)$$

that shows the closeness of the experimental condition for the best one.

Step 9: Ranking the experimental conditions with the increasing d_i. The condition with the smallest d_i should be ranked first and may be chosen as the optimized experimental condition.

An example of three experimental conditions with three output responses $R = [r_{ij}]$ is shown below. The decision matrix and normalized decision matrix for this study are shown in Table 5.

Calculated weighted normalized decision matrix, proximity index values, and overall proximity indexed values and ranks are shown in Table 6.

Table 5 – Decision matrix and normalized decision matrix of responses

Exp. no	Decision matrix values			Normalized decision matrix values		
	A	B	C	A	B	C
1	2.16	2.15	143.50	0.278	0.250	0.135
2	2.19	2.17	246.00	0.444	0.333	0.300
3	2.20	2.25	398.50	0.500	0.714	0.546
4	2.21	2.26	522.50	0.556	0.762	0.745
5	2.21	2.36	680.50	0.556	1.238	1.000
6	2.14	2.14	103.00	0.167	0.190	0.069
7	2.15	2.14	220.00	0.222	0.190	0.258
8	2.16	2.15	334.00	0.278	0.238	0.442
9	2.17	2.15	455.50	0.333	0.238	0.637
10	2.21	2.15	586.00	0.556	0.238	0.848
11	2.14	2.13	108.50	0.167	0.143	0.078
12	2.14	2.14	203.00	0.167	0.190	0.230
13	2.15	2.14	308.00	0.222	0.190	0.400
14	2.16	2.15	406.50	0.278	0.238	0.558
15	2.20	2.15	487.50	0.500	0.238	0.689
16	2.12	2.13	67.00	0.056	0.143	0.011
17	2.14	2.14	94.50	0.167	0.190	0.056
18	2.16	2.16	145.50	0.278	0.286	0.138
19	2.18	2.17	209.50	0.389	0.333	0.241
20	2.22	2.23	255.00	0.611	0.619	0.314
21	2.13	2.11	61.50	0.111	0.048	0.002
22	2.17	2.15	96.50	0.333	0.238	0.059
23	2.21	2.23	136.50	0.556	0.619	0.123
24	2.26	2.28	180.50	0.833	0.857	0.194
25	2.29	2.31	246.00	1.000	1.000	0.300

Table 6 – Weighted normalized decision matrix, proximity index values, and overall proximity indexed values and ranks

Exp. no	Weighted normalized decision matrix values			Proximity indexed values			Over proximity indexed values	Rank
1	0.0612	0.0825	0.0608	0.0489	0.2028	0.0599	0.3115	9
2	0.0977	0.1099	0.1350	0.0854	0.2858	0.1341	0.5053	15
3	0.1100	0.2356	0.2457	0.0977	0.6668	0.2448	1.0093	21
4	0.1223	0.2515	0.3353	0.1100	0.7148	0.3344	1.1592	23
5	0.1223	0.4085	0.4500	0.1100	1.1908	0.4491	1.7499	25
6	0.0367	0.0627	0.0311	0.0244	0.1428	0.0302	0.1974	5
7	0.0488	0.0627	0.1161	0.0365	0.1428	0.1152	0.2945	8
8	0.0612	0.0785	0.1989	0.0489	0.1908	0.1980	0.4377	12
9	0.0733	0.0785	0.2867	0.0610	0.1908	0.2858	0.5375	16
10	0.1223	0.0785	0.3816	0.1100	0.1908	0.3807	0.6815	18
11	0.0367	0.0472	0.0351	0.0244	0.0958	0.0342	0.1544	3
12	0.0367	0.0627	0.1035	0.0244	0.1428	0.1026	0.2698	6
13	0.0488	0.0627	0.1800	0.0365	0.1428	0.1791	0.3584	11
14	0.0612	0.0785	0.2511	0.0489	0.1908	0.2502	0.4899	14
15	0.1100	0.0785	0.3101	0.0977	0.1908	0.3092	0.5977	17
16	0.0123	0.0472	0.0050	0.0000	0.0958	0.0041	0.0999	2
17	0.0367	0.0627	0.0252	0.0244	0.1428	0.0243	0.1915	4
18	0.0612	0.0944	0.0621	0.0489	0.2388	0.0612	0.3489	10
19	0.0856	0.1099	0.1085	0.0733	0.2858	0.1076	0.4666	13
20	0.1344	0.2043	0.1413	0.1221	0.5718	0.1404	0.8343	20
21	0.0244	0.0158	0.0009	0.0121	0.0008	0.0000	0.0129	1
22	0.0733	0.0785	0.0266	0.0610	0.1908	0.0257	0.2744	7
23	0.1223	0.2043	0.0554	0.1100	0.5718	0.0545	0.7363	19
24	0.1833	0.2828	0.0873	0.1710	0.8098	0.0864	1.0672	22
25	0.2200	0.3300	0.1350	0.2077	0.9528	0.1341	1.2946	24

Examining the relative importance of drilling elements for the different performance characteristics is still necessary to precisely determine the best combinations of drilling parameters. The results are analyzed using the variance analysis. Using an analysis of variance (ANOVA), it was possible to determine which drilling variables significantly affect performance metrics. The whole variability of the entropy-based proximity index values is split. Doing this separates the contributions from each drilling variable and error from the total sum of the squared deviations of the Grey relational grade. The F-test may also be run to determine which machining conditions substantially impact drilling performance. Changing the drilling parameter influences performance attributes when *F* is substantial. In addition, an estimation of the percentage of influence is provided to analyze the major variables and how they affect composite machining.

Table 7 indicates that the F value of the feed rate is 15.89, more significant than the spindle speed of 8.02.

Table 7 – ANOVA for entropy-based proximity indexed value

Source	*DF*	Sum of squares	Mean square	*F*	% contribution	*P*
Speed	4	1.2226	0.30564	8.02	28.74	0.001
Feed	4	2.4219	0.60547	15.89	56.93	0.000
Error	16	0.6096	0.03810	–	14.33	–
Total	24	4.2540	–	–	–	–

5 Discussion

Researchers utilize many methodologies to maximize multiple performance metrics: desirability approach, grey relational analysis and utility concept, grey relational analysis and fuzzy logic, and grey entropy fuzzy methods.

Unlike other studies, this one used a hybrid approach called the entropy-based weight integrated proximity indexed value method to determine the ideal drilling settings for this multiple response optimization.

This combines the proximity-indexed value method and the entropy approach used to calculate the response weights.

This study discusses the multi-response drilling optimization of GFRP laminate using a novel approach that combines fuzzy logic, gray relational analysis, and the entropy method for weights.

The data presented in Table 7 is consistent with the findings of Palanikumar [9]. The feed rate is the variable that, when drilling GFRP laminate, most affects thrust force and delamination variables. In this current study, the percentage error is 14.33. However, in a similar study by Palanikumar [9], it was 14.78. The new work's accuracy and reduced percentage error can be attributed to using a more significant number of levels.

Experiment no. 21 shows that the ideal combination of input parameters (speed 2500 rpm, feed 50 mm/min) for multi-response optimization has the smallest value E-PIV of 0.0129.

6 Conclusions

Feed and speed are factors, whereas torque, thrust force, entry/peel-up, and exit/push-out delamination factors are responses. Based on the findings, the following conclusions are made.

The findings indicate that an increase in feed rate results in an increase in delamination and thrust force.

As the spindle speed increased, there was a modest drop in the delamination factor, torque, and thrust force.

A lower proximity index value indicates higher performance. Therefore, drilling with core drill at 2500 rpm and feed at 50 mm/min produces less delamination and thrust force.

The experiment's findings suggest that selecting drilling parameters enhances drilling performance.

According to the ANOVA, feed is the drilling variable that has the most significant impact on the E-PIV. Spindle speed has a lesser influence on drilling performance.

Nevertheless, the following are the limitations of this study. Although PIV works effectively in certain situations, its efficacy varies depending on the issue and may not always produce consistent outcomes. The PIV method seeks to reduce rank reversal in settings involving multiple criteria decision-making (MCDM). Other research, however, also indicates that rank reversal is still quite common under the PIV approach. This indicates that while it makes an effort to address the problem, it is not resolved entirely.

Also, by adding criteria weight calculation utilizing techniques like CRITIC and WENSLO to the recently discovered MCDM methods like MABAC, MAIRCA, and FUCOM, future research can concentrate on optimizing machining parameters.

References

1. Khashaba, U.A. Othman, R. (2017). Low-velocity impact of woven CFRE composites under different temperature levels. *International Journal of Impact Engineering*, Vol. 108, pp. 191–204. https://doi.org/10.1016/j.ijimpeng.2017.04.023
2. Shin, L.J., Dassan, E.G.B., Abidin, M.S.Z., Anjang, A. (2020). Tensile and compressive properties of glass fiber-reinforced polymer hybrid composite with eggshell powder. *Arabian Journal for Science and Engineering*, Vol. 45, pp. 5783–5791. https://doi.org/10.1007/s13369-020-04561-z
3. Reisgen, U., Schiebahn, A., Lotte, J., Hopmann, C., Schneider, D., Neuhaus, J. (2020). Innovative joining technology for the production of hybrid components from FRP and metals. *Journal of Materials Processing Technology*, Vol. 282, 116674. https://doi.org/10.1016/j.jmatprotec.2020.116674
4. Bayraktar, S., Turgut, Y. (2020). Determination of delamination in drilling of carbon fiber reinforced carbon matrix composites/Al 6013-T651 stacks. *Measurement*, Vol. 154, 107493. https://doi.org/10.1016/j.measurement.2020.107493
5. Masoud, F., Sapuan, S.M., Ariffin, M.K.A.M., Nukman, Y., Bayraktar, E. (2020). Cutting processes of natural fiber-reinforced polymer composites. *Polymers*, Vol. 12(6), 1332. https://doi.org/10.3390/polym12061332
6. Babu, J., Sunny, T., Paul, N.A., Mohan, K.P., Philip, J., Davim, J.P. (2016) Assessment of delamination in composite materials: A review. *Proceedings of the Institution of Mechanical Engineers, Part B: Journal of Engineering Manufacture*, Vol. 230(11), pp. 1990–2003. https://doi.org/10.1177/0954405415619343
7. Babu, J., Philip, J., Zacharia, T., Davim, J.P. (2015) Delamination in composite materials: measurement, assessment and prediction. In: Davim J.P. et al. (eds) *Machinability of Fibre-Reinforced Plastics*, pp. 139–162. De Gruyter, Berlin. https://doi.org/10.1515/9783110292251-006
8. Sobri, S.A., Whitehead, D., Mohamed, M., Mohamed, J.J., Amini, M.H.M., Hermawan, A., Rasat, M.S.M., Sofi, A.Z.M., Ismail, WOASW, Norizan, M.N. (2020). Augmentation of the delamination factor in drilling of carbon fibre-reinforced polymer composites (CFRP). *Polymers*, Vol. 12(11), 2461. https://doi.org/10.3390/polym12112461
9. Khashaba, U.A., Abd-Elwahed, M.S., Ahmed, K.I., Najjar, I., Melaibari, A., Eltaher, M.A. (2020) Analysis of the machinability of GFRE composites in drilling processes. *Steel and Composite Structures*, Vol. 36, pp. 417–426. https://doi.org/10.12989/scs.2020.36.4.417
10. Khashaba, U.A., El-Keran, A.A. (2017). Drilling analysis of thin woven glass-fiber reinforced epoxy composites. *Journal of Materials Processing Technology*, Vol. 249, pp. 415–425. https://doi.org/10.1016/j.jmatprotec.2017.06.011
11. Formisano, A., Papa, I., Lopresto, V., Langella, A. (2019). Influence of the manufacturing technology on impact and flexural properties of GF/PP commingled twill fabric laminates. *Journal of Materials Processing Technology*, Vol. 274, 116275. https://doi.org/10.1016/j.jmatprotec.2019.116275
12. Erturk, A.T., Vatansever, F., Yarar, E., Guven, E.A., Sinmazcelik, T. (2021). Effects of cutting temperature and process optimization in drilling of GFRP composites. *Journal of Composite Materials*, Vol. 55(2), pp. 235–249.
13. Ramesh, B., Elayaperumal, A., Satishkumar, S., Kumar, A. (2018). Drilling of pultruded and liquid composite moulded glass/epoxy thick composites: Experimental and statistical investigation. *Measurement*, Vol. 114, pp. 109–121. https://doi.org/10.1016/j.measurement.2017.09.026
14. Qiu, X., Li, P., Li, C., Niu, Q., Chen, A., Ouyang, P., Ko, T.J. (2018). Study on chisel edge drilling behavior and step drill structure on delamination in drilling CFRP. *Composite Structures*, Vol. 203, pp. 404–413. https://doi.org/10.1016/j.compstruct.2018.07.007

15. Giasin, K., Gorey, G., Byrne, C., Sinke, J., Brousseau, E. (2019). Effect of machining parameters and cutting tool coating on hole quality in dry drilling of fibre metal laminates. *Composite Structures*, Vol. 212, pp. 159–174. https://doi.org/10.1016/j.compstruct.2019.01.023
16. Xu, J., Li, C., Chen, M., El Mansori, M., Davim, J.P. (2020). On the analysis of temperatures, surface morphologies and tool wear in drilling CFRP/Ti6Al4V stacks under different cutting sequence strategies. *Composite Structures*, Vol. 234(15), 111708. https://doi.org/10.1016/j.compstruct.2019.111708
17. Fu, R., Jia, Z., Wang, F., Jin, Y., Sun, D., Yang, L., Cheng, D. (2018). Drill-exit temperature characteristics in drilling of UD and MD CFRP composites based on infrared thermography. *International Journal of Machine Tools and Manufacture*, Vol. 135, pp. 24–37. https://doi.org/10.1016/j.ijmachtools.2018.08.002
18. Xu, W., Zhang, L. (2019). Heat effect on the material removal in the machining of fibre-reinforced polymer composites. *International Journal of Machine Tools and Manufacture*, Vol. 140, pp. 1–11. https://doi.org/10.1016/j.ijmachtools.2019.01.005
19. Zhang, B., Wang, F., Wang, Q., Zhao, X. (2021). Novel fiber fracture criteria for revealing forming mechanisms of burrs and cracking at hole-exit in drilling carbon fiber reinforced plastic. *Journal of Materials Processing Technology*, Vol. 289, 116934. https://doi.org/10.1016/j.jmatprotec.2020.116934
20. Zhang, B., Wang, F., Wang, X., Li, Y., Wang, Q. (2020). Optimized selection of process parameters based on reasonable control of axial force and hole-exit temperature in drilling of CFRP. *The International Journal of Advanced Manufacturing Technology*, Vol. 110, pp. 797–812. https://doi.org/10.1007/s00170-020-05868-9
21. Wang, F.J., Zhao, M., Fu, R., Yan, J.B., Qiu, S., Hao, J.X. (2021). Novel chip-breaking structure of step drill for drilling damage reduction on CFRP/Al stack. *Journal of Materials Processing Technology*, Vol. 291, 117033. https://doi.org/10.1016/j.jmatprotec.2020.117033
22. Bai, Y., Jia, Z.Y., Fu, R., Hao, J.X., Wang, F.J. (2021). Mechanical model for predicting thrust force with tool wear effects in drilling of unidirectional CFRP. *Composite Structures*, Vol. 262(4) 113601. https://doi.org/10.1016/j.compstruct.2021.113601
23. Jia, Z.Y., Zhang, C., Wang, F.J., Fu, R., Chen, C. (2020). Multi-margin drill structure for improving hole quality and dimensional consistency in drilling Ti/CFRP stacks. *Journal of Materials Processing Technology*, Vol. 276, 116405. https://doi.org/10.1016/j.jmatprotec.2019.116405
24. Jia, Z., Chen, C., Wang, F., Zhang, C. (2020). Analytical study of delamination damage and delamination-free drilling method of CFRP composite. *Journal of Materials Processing Technology*, Vol. 282, 116665. https://doi.org/10.1016/j.jmatprotec.2020.116665
25. Rahmé, P., Moussa, P., Lachaud, F., Landon, Y. (2020). Effect of adding a woven glass ply at the exit of the hole of CFRP laminates on delamination during drilling. *Composites Part A: Applied Science and Manufacturing*, Vol. 129, 105731. https://doi.org/10.1016/j.compositesa.2019.105731
26. Galińska, A. (2020). Mechanical joining of fibre reinforced polymer composites to metals – A review. Part I: Bolted joining. *Polymers*, Vol. 12(10), 2252. https://doi.org/10.3390/polym12102252
27. Ramesha, K., Santhosh, N., Kiran, K., Manjunath, N., Naresh, H. (2019). Effect of the process parameters on machining of GFRP composites for different conditions of abrasive water suspension jet machining. *Arabian Journal for Science and Engineering*, Vol. 44, pp. 7933–7943. https://doi.org/10.1007/s13369-019-03973-w
28. Grilo, T.J., Paulo, R.M.F., Silva, C.R.M., Davim, J.P. (2013). Experimental delamination analyses of CFRPs using different drill geometries. *Composites Part B: Engineering*, Vol. 45, pp. 1344–1350. https://doi.org/10.1016/j.compositesb.2012.07.057
29. Ismail, S.O., Dhakal, H.N., Dimla, E., Popov, I. (2017). Recent advances in twist drill design for composite machining: A critical review. *Proceedings of the Institution of Mechanical Engineers, Part B: Journal of Engineering Manufacture*, Vol. 231(14), pp. 2527–2542. https://doi.org/10.1177/0954405416635034
30. Geng, D., Liu, Y., Shao, Z., Lu, Z., Cai, J., Li, X., Zhang, D. (2019). Delamination formation, evaluation and suppression during drilling of composite laminates: A review. *Composite Structures*, Vol. 216, pp. 168–186. https://doi.org/10.1016/j.compstruct.2019.02.099
31. Durão, L.M.P., Gonçalves, D.J., Tavares, J.M.R., de Albuquerque, V.H.C., Vieira, A.A., Marques, A.T. (2010). Drilling tool geometry evaluation for reinforced composite laminates. *Composite Structures*, Vol. 92, pp. 1545–1550. https://doi.org/10.1016/j.compstruct.2009.10.035
32. Kilickap, E. (2010). Optimization of cutting parameters on delamination based on Taguchi method during drilling of GFRP composite. *Expert Systems with Applications*, Vol. 37 pp. 6116–6122. https://doi.org/10.1016/j.eswa.2010.02.023
33. Díaz-Álvarez, A., Díaz-Álvarez, J., Santiuste, C., Miguélez, M.H. (2019). Experimental and numerical analysis of the influence of drill point angle when drilling bio-composites. *Composite Structures*, Vol. 209, pp. 700–709. https://doi.org/10.1016/j.compstruct.2018.11.018
34. Ismail, S.O., Ojo, S.O., Dhakal, H.N. (2017). Thermo-mechanical modelling of FRP cross-ply composite laminates drilling: Delamination damage analysis. *Composites Part B: Engineering*, Vol. 108, pp. 45–52. https://doi.org/10.1016/j.compositesb.2016.09.100
35. Arrospide, E., Bikandi, I., Larrañaga, I., Cearsolo, X., Zubia, J., Durana, G. (2019). Harnessing deep-hole drilling to fabricate air-structured polymer optical fibres. *Polymers*, Vol. 11(11), 1739. https://doi.org/10.3390/polym11111739

36. Liu, S., Yang, T., Liu, C., Jin, Y., Sun, D., Shen, Y. (2020). Mechanistic force modelling in drilling of AFRP composite considering the chisel edge extrusion. *The International Journal of Advanced Manufacturing Technology*, Vol. 109, pp. 33–44. https://doi.org/10.1007/s00170-020-05608-z
37. Qiu, X., Li, P., Li, C., Niu, Q., Chen, A., Ouyang, P., Ko, T.J. (2019). New compound drill bit for damage reduction in drilling CFRP. *International Journal of Precision Engineering and Manufacturing-Green Technology*, Vol. 6, pp. 75–87. https://doi.org/10.1007/s40684-019-00026-3
38. Hocheng, H., Tsao, C.C. (2003). Analysis of delamination in drilling composite materials using core drill. *Applied Mechanics*, Vol. 2002, pp. 285–290. https://doi.org/10.1142/9789812777973_0046
39. Hocheng H., Tsao, C.C. (2006). Effects of special drill bits on drilling-induced delamination of composite materials. *International Journal of Machine Tools and Manufacture*, Vol. 46(12–13), pp. 1403–1416. https://doi.org/10.1016/j.ijmachtools.2005.10.004
40. Tsao, C.C. (2006). The effect of pilot hole on delamination when core drill drilling composite materials. *International Journal of Machine Tools and Manufacture*, Vol. 46(12–13), pp. 1653–1661. https://doi.org/10.1016/j.ijmachtools.2005.08.015
41. Nekrasov, S., Zhyhylii, D., Dovhopolov, A., Karatas, M.A. (2021) Research on the manufacture and strength of the innovative joint of FRP machine parts, *Journal of Manufacturing Processes*, Vol. 72, pp. 338–349. https://doi.org/10.1016/j.jmapro.2021.10.025
42. Wang, H., Zhang, X., Duan, Y. (2022) Investigating the Effect of low-temperature drilling process on the mechanical behavior of CFRP. *Polymers*, Vol. 14(5), 1034. https://doi.org/10.3390/polym14051034
43. Wu, T., Kruse, R., Tinkloh, S., Tröster, T., Zinn, W., Lauhoff, C., Niendorf, T. (2022). Experimental analysis of residual stresses in CFRPs through hole-drilling method: The role of stacking sequence, thickness, and defects. *Journal of Composites Science*, Vol. 6(5), pp. 131–138. https://doi.org/10.3390/jcs6050138
44. Babu, J., Alex N.P., Abraham, S.P., Philip J., Anoop B.N., Davim J.P. (2018). Development of a comprehensive delamination assessment factor and its evaluation with high-speed drilling of composite laminates using a twist drill. *Proceedings of the Institution of Mechanical Engineers, Part B: Journal of Engineering Manufacture*, Vol. 232(12), pp. 2109-2121. https://doi.org/10.1177/0954405417690552
45. Mufazzal, S., Muzakkir, S.M. (2018). A new multi-criterion decision making (MCDM) method based on proximity indexed value for minimizing rank reversals. *Computers & Industrial Engineering*, Vol. 119, pp. 427–438. https://doi.org/10.1016/j.cie.2018.03.045
46. Raigar, J., Sharma, V.S., Srivastava, S., Chand, R., Singh, J. (2020). A decision support system for the selection of an additive manufacturing process using a new hybrid MCDM technique. *Sādhanā*, Vol. 45, 101. https://doi.org/10.1007/s12046-020-01338-w
47. Babu, J., Anjaiah, M., Sunny, T., Ramana, M.V. (2022). Multi characteristic optimization of high-speed machining of GFRP laminate by hybrid Taguchi desirability approach. *Materials Today: Proceedings*, Vol. 58(1), pp. 238–241. https://doi.org/10.1016/j.matpr.2022.02.097
48. Ajith, S., Sharma V.S., Bharath, N., Babu, J., Balasubramanyan, R. (2022). A decision support system for materials selection using proximity indexed value method. *Materials Today: Proceedings*, Vol. 66(4), pp. 2431–2437. https://doi.org/10.1016/j.matpr.2022.06.341